Transmission Electron Microscopic and X-ray Diffraction Based Crystallographic Bibliography Comparison of Silver, Copper and Titanium Functional Nanocrystals: A Statical Review

ABSTRACT

This statistical review compares the crystallographic structures of functional nanocrystals composed of silver, copper and titanium using transmission electron microscopy (TEM) and X-ray diffraction (XRD) analyses. TEM provides high-resolution imaging to directly visualize the size, shape, and crystallinity of individual nanoparticles. XRD reveals the crystal phases, lattice parameters, and crystallite sizes averaged over the bulk nanocrystal samples. By combining these complementary techniques, a comprehensive assessment is made of the crystallographic characteristics influencing the functional properties of these metallic nanocrystal systems. Statistical analyses quantify variations in crystal structure, size distributions, phase compositions, lattice strains, and lattice volume of these three crystalline nanomaterials. Correlations are drawn between crystallographic features and the nanocrystal's electronic, catalytic, corrosion-resistant and antimicrobial behaviors. This quantitative comparison provides valuable insights into the structure-property relationships in these functional nanocrystals, enabling rational design strategies for optimizing their performance in various applications. The review highlights the complementary roles of TEM and XRD in comprehensive nanocrystal characterization.

Keywords: Crystallographic bibliography, nanocrystals, phase, transmission electron microscopic, x-ray diffraction.

1.0 Introduction

The accurate characterization and comparison of functional nanocrystals is essential to the advancement of many technological applications in the field of nanotechnology [1]. Nanomaterials are very beneficial because of their great catalytic activity, decreased size and enhanced solubility [1]. Materials with a crystalline arrangement of atoms or molecules that are structured at the nanoscale are known as crystalline nanomaterials [2]. Due to their diminutive dimensions and expansive surface area, they often exhibit unique properties that render them valuable across diverse sectors such as electronics, healthcare, and energy storage [2]. The mechanical strength, wide surface area, superior electrical conductivity, customizable optical qualities, thermal stability and conductivity and customizable chemical reactivity are just a few of the benefits that crystalline nanostructures have to offer [2]. Nanomaterials can have extraordinary mechanical qualities including high strength and stiffness, because of their crystalline structure, which is useful for structural applications [3].

Compared to their bulk equivalents, certain nanomaterials exhibit better thermal stability and conductivity [4]. The chemical reactivity of nanoparticles can be precisely controlled using surface functionalization and modification approaches [4]. Because of these characteristics, crystalline nanomaterials are very adaptable and sought after for a variety of technological uses [4]. Crystalline nanomaterials are important in many sectors because of their special characteristics at the nanoscale [5]. By adjusting the nanomaterial's size, shape and composition these qualities can be customized [5]. They make it possible to create new materials with improved optical, magnetic, electrical and mechanical characteristics [5]. It is possible to precisely customize their size and form to maximize stability, selectivity and catalytic activity [5]. Their special qualities can improve the efficiency, stability and performance of devices [5]. They are efficient at removing impurities from air and water due to their high surface area and

reactivity [5]. Additionally, because of their small size, they can interact with biological systems at the molecular and cellular levels, resulting in treatments that are effective and precisely targeted [5]. Methods such as X-ray diffraction (XRD) which offer insights into crystal structure and lattice parameters are widely employed for the characterization of the crystalline properties of silver nanoparticles [6, 7]. Depending on variables including synthesis conditions and method, silver nanoparticles can exhibit various crystalline configurations including face-centered cubic (FCC) or hexagonal close-packed (HCP) structures. [6, 7]. Their applications in areas like biomedical technology, sensing and catalysis are impacted by these features, which also affect their physical, chemical and optical behaviour [6, 7]. The synthesis process and circumstances of copper nanoparticles can influence their crystalline characteristics [8]. They usually have a crystalline structure depending on their size, shape and surface characteristics [8]. The arrangement can be either body-centered cubic (BCC) or face-centered cubic (FCC) in this structure [8]. Their chemical and physical characteristics, including mechanical strength, conductivity and catalytic activity are influenced by their crystallinity [8].

Certain characteristics of titanium nanoparticles like size, surface treatment and production method can lead to crystalline qualities [9]. Their optical behaviour, mechanical strength and chemical reactivity can all be impacted by these characteristics [9]. Titanium nanoparticles can have a variety of crystalline forms including anatase, rutile or anatase-rutile mixed phases depending on the production method [9]. Their performance in a variety of applications including energy storage, biomedical devices and catalysis is impacted by these architectures [9]. Nanoparticles made of titanium, copper and silver each have special qualities and uses [10]. Due to their well-known antibacterial qualities, silver nanoparticles are beneficial in consumer goods and medical equipment [10]. Copper nanoparticles are useful in electronics, catalysis and they also show antibacterial properties [11]. Titanium nanoparticles are used in sunscreen, medical implants and aircraft because of their strength, lightweight and corrosion resistance [11].

Excellent optical qualities are characteristic of silver nanoparticles [12]. Strong mechanical properties characterize copper nanoparticles [12]. Titanium nanoparticles are recognized for their high strength-to-weight ratio, corrosion resistance and compatibility with biological systems [12]. The reactivity of silver nanoparticles is high [13]. Certain acids and oxidizing substances cause copper nanoparticles to react [13]. In general, titanium nanoparticles are less reactive than those of silver and copper, although at high temperatures they can react with strong acids and bases [13]. Silver nanoparticles are widely employed in electronics, catalysts, antimicrobial coatings and wound dressings [14]. Copper nanoparticles find applications in catalysts, antimicrobial surfaces, printed electronics and conductive inks [14]. Titanium nanoparticles find application in water purification systems, sunscreen formulations, medicinal implants and aeronautical materials [14].

Since silver nanoparticles are widely used in consumer goods, there are worries over their possible harm to people and ecosystems [15]. Nanoparticles of copper are vital trace elements for many species of copper [15]. Although long-term consequences are still being investigated, titanium nanoparticles are generally considered safer than copper and silver nanoparticles [15]. As silver is more expensive than copper and titanium, silver nanoparticles are rather pricey [16]. Compared to silver, copper nanoparticles are more affordable and more widely available [16]. Because of their energy-intensive manufacturing method, titanium nanoparticles can be expensive; nevertheless, their availability depends on demand and manufacturing capacity [16]. We hope to clarify the similarities and contrasts between these materials' crystallographic properties through a thorough statistical analysis, providing insight into their uses and directing future research activities.

2.0 Materials and Methods

Three essential ingredients are required to acquire nanoparticles, particularly copper nanoparticles. Initially, a substance that releases ions. Furthermore, the acquisition of atoms needs the presence of a reducing agent to furnish electrons. Under optimal temperature and pH circumstances, the surfactant facilitates the aggregation of atoms the reducing agent produces into nanoparticles. Diverse metallic nanoparticles can be synthesized using various physical, chemical, and biological techniques [32]. Chemical methods provide precise control over the size, growth, shape, and dispersion of particles by optimizing reaction parameters, including reaction duration, pH, and choice of solvent. So, chemical methods like sol-gel, chemical reduction, microwave-assisted, hydrothermal etc are mentioned in this manuscript. Nanoparticles have been synthesized via a variety of methods with different precursorsfor titanium nanoparticles precursors like titanium tetrachloride ($TiCl_4$), Titanium isopropoxide (TTIP), Tetrabutyl Titanate;for silver nanoparticle precursors like $AgNO_3$; for copper nanoparticles precursors like $CuSO_4$, Cu $(NO_3)_2$, $CuCl_2$ etc are used.

Table 1. Various methods for Ag, Cu and TiO_2 production.

Methods	Precursors	Conditions	References
Crystalline Silver nanoparticles			
Sol-Gel	TEOS (Tetraethyl orthosilicate), $AgNO_3$	Solvent: Ethanol (Exerting Nitric acid promotes hydrolysis). Ratio- TEOS: Ethanol: H_2O = 1:4:4.	[17]
Chemical reduction	$AgNO_3$	Solvent: Water. Reducing agent: Ascorbic acid. Stabilizer: PVP. Temperature: 80.0 ^{0}C, 12.0 h.	[18]
Ultrasound irradiation	$AgNO_3$	Solvent: Water. Reducing and stabilizing agent: Fructose and starch.	[19]
Hydrothermal	$AgNO_3$	Two ion exchange processes: 1) Chabazite tuff with NH_4^+ 2) Latter ions change with silver Temperature: 400.0 ^{0}C, 1h.	[20]
Crystalline Copper nanoparticles			

Wet chemical	$CuSO_4$	Solvent: Water or Ethylene glycol. Reducing agent: Ascorbic acid. Stabilizer: PVP. Temperature: 80.0 ^{0}C.	[21]
Wet chemical	$CuCl_2$	Solvent: Ethanol. Reducing agent: $NaBH_4$. Stabilizer: PVP. Sealed for 8.0 h.	[22]
Wet chemical	Cu $(NO_3)_2$	Solvent: Water + Ethylene glycol. Reducing agent: $NaBH_4$. Stabilizer: Tergitol NP-9. Temperature: Room temp, 2.0 h.	[23]
Microwave-assisted	$CuSO_4.5H_2O$	Solvent: Ethylene glycol. Reducing agent: $NaH_2PO_2.H_2O$. Stabilizer: PVP.	[24]
Sonochemical	$CuSO_4$	Solvent: Water. Reducing agent: Na_2H_4. Stabilizer: PVP.	[25]
Microwave	$CuCl_2$	Solvent: Water + Ethylene glycol. Reducing agent: Ethylene glycol + H_2. Stabilizer: Sodium laurate.	[26]
Crystalline Titanium nanoparticles			
Sol-Gel	Ti $(OH)_4$	Solvent: Basic medium. Triethanolamine increases the nucleation rate. Temperature: 100.0 ℃, 24.0 h and 140.0 ℃, 72.0 h.	[27]
Co-precipitation	TTIP	Solvent: A mixture of methanol and ethanol. Calcinated below 500.0 ℃. Temperature: Room temperature.	[28]
Hydrothermal	Pure TiO_2	Solvent: NaOH and KOH. Calcinated at 250.0 ℃, 2.0 h. Temperature: 200.0 ℃, 48.0 h.	[29]
Solvothermal	Tetrabutyl Titanate	Both oleic acid and dodecyl amine performed as capping surfactants. Temperature: 300.0 ℃, 10.0 h.	[30]
Wet chemical	$TiCl_4$	Solvent: HCl Polyethylene glycol (PEG-1000) was used. Temperature: 80.0 ℃, 2.0 h.	[31]

3.0 Characterization

The crystallographic textures of any nanocrystal were investigated by XRD and TEM which were explored [33-37] in Table 2.

Table 2. Crystallographic bibliographic parameters of silver, copper and titanium nanocrystals

Sl No.		Crystallographic bibliography parameters	Reference
01.	XRD	Lattice parameters, axial parameters, angular parameters, strain, lattice volume, microstrain, crystal structure, crystal shape, preferred orientation, crystallinity, crystal size, interplanar distance and crystal plane or miller indices.	[33-34]
02.	TEM	Internal morphology, strain, defect, orientation, shape, structure, volume fraction, axial parameters, angular parameters, selected area diffraction plane or Miller indices, nanobeam diffraction onto the plane, the stress of crystal, preferred orientation, grain boundary, particle sizes and dislocation density of nanocrystals.	[34-37]

4.0 Results and Discussions

4.1. X-ray diffraction (XRD) Analysis

X-ray diffraction (XRD) analysis is an effective method employed for examining the crystal structure of materials including Ag, Cu and Ti crystals [38]. When X-ray radiation strikes a crystalline substance, it interacts with the atoms within the crystal lattice planes, leading to constructive and destructive interference patterns [38]. These interference patterns are recorded as diffraction peaks, which can be analyzed to determine various structural properties of the material [39]. The locations and strengths of the diffraction pattern can be utilized to ascertain both the crystal system and the lattice parameters of the crystals [39]. The widening of the diffraction pattern can be attributed to the limited size of the crystallites and the existence of strain within the crystal lattice [39].In a pure silver (Ag) crystal, the X-ray diffraction (XRD) pattern will exhibit distinct peaks corresponding to the different crystallographic planes present in the crystal structure. The XRD pattern of a pure Ag crystal is characteristic of its face-centered cubic (FCC) crystal structure **(Fig. 2)** [40]. In the XRD pattern of pure silver crystals, the most

notable peaks are typically observed at the following positions (expressed in terms of the Miller indices (hkl) and the corresponding interplanar spacing (d) values): (111) plane: d = 2.359 Å, (200) plane: d = 2.044 Å, (220) plane: d = 1.445 Å, (311) plane: d = 1.231 Å, (222) plane: d = 1.179 Å [41-42]. The relative intensities of these peaks follow a pattern that is determined by the structure factor and the multiplicity of the planes [43]. In the case of an FCC crystal like Ag, the most intense peak typically corresponds to the (111) plane, followed by the (200), (220), (311), and (222) planes in decreasing order of intensity **(Fig. 1).**The most prominent peaks in the XRD pattern of pure silver are (111) plane: $2\theta \approx 38.1°$, (200) plane: $2\theta \approx 44.3°$, (220) plane: $2\theta \approx 64.4°$ [43-45].The X-ray diffraction (XRD) pattern obtained from a pure copper (Cu) crystal is characterized by distinct reflection corresponding to the different crystallographic planes present in the face-centered cubic (FCC) structure of copper (**Fig. 2**) [46].

The primary peaks in the XRD pattern of a pure copper crystal are commonly detected at the following angles (2θ values) and corresponding crystallographic planes: 43.3° (111) plane, 50.4° (200) plane, 74.1° (220) plane, 89.9° (311) plane, 95.1° (222) plane [46-47, 49]. The relative intensities of these peaks follow the pattern: (111) > (200) > (220) > (311) > (222) **(Fig.1)** [48]. The XRD pattern of pure Cu crystal also exhibits additional peaks at higher angles, corresponding to other crystallographic planes, but with lower intensities [48].The X-ray diffraction (XRD) profile of a pure titanium (Ti) crystal depends on its crystal structure and lattice parameters [50]. At room temperature, titanium possesses a hexagonal close-packed (HCP) crystal structure, commonly referred to as the alpha (α) phase and its XRD pattern will exhibit characteristic peaks corresponding to the allowed diffraction planes in the HCP structure **(Fig. 2)** [50]. The most prominent peaks in the XRD pattern of pure Ti crystal are typically observed at the following 2θ (Bragg) angles: (100) plane: $2\theta \approx 35.1°$, (002) plane: $2\theta \approx 38.4°$, (101) plane: $2\theta \approx 40.2°$, (102) plane: $2\theta \approx 53.0°$, (103) plane: $2\theta \approx 63.0°$, (110) plane: $2\theta \approx 70.7°$, (112) plane: $2\theta \approx$

76.2°, (201) plane: $2\theta \approx 82.3°$ [51-53]. The relative intensities of these peaks, as well as the presence of additional peaks at higher angles, can provide information about the preferred orientation (texture) and crystallographic purity of the titanium crystal [55]. Additionally, the Ti sample may experience a phase shift to the beta (β) phase, also known as the body-centered cubic (BCC) structure, if it is exposed to high temperatures or specific heat treatments [54]. In these situations, distinct peaks that correspond to the β-Ti phase would be visible in the XRD pattern [54].

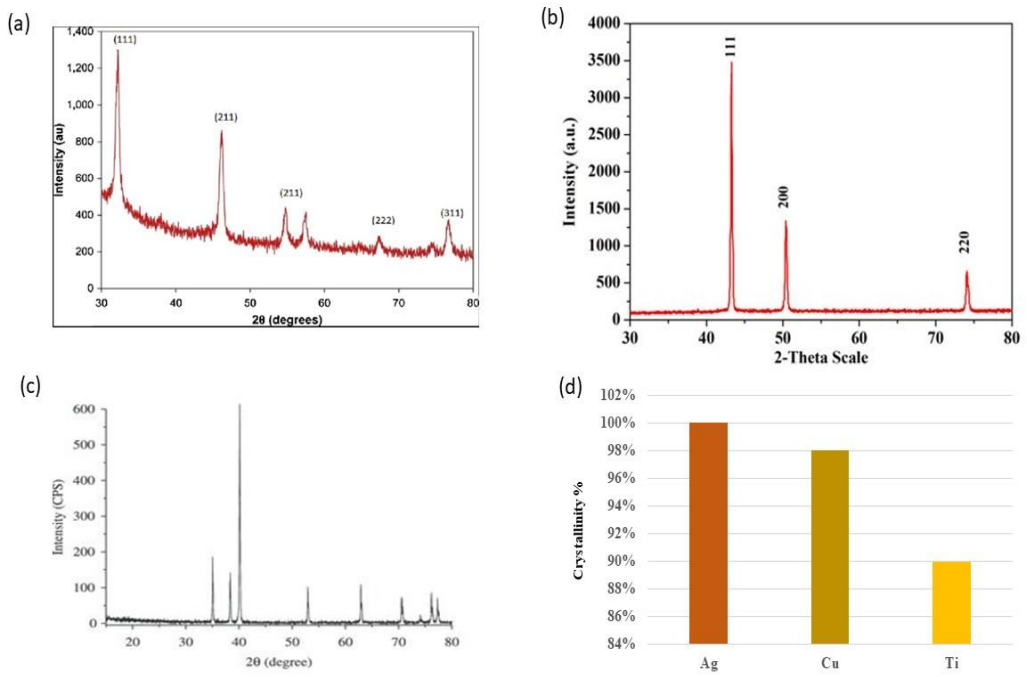

Fig. 1. (a) XRD profile of pure Ag crystals [56]; (b) XRD patterns of pure Cu crystals [57]; (c) XRD patterns of pure Ti crystals [58]; (d) Relative crystallinity of Ag, Cu and Ti [59-61].

The percentage of crystallinity, or the degree of crystallinity, refers to the fraction of a material that is crystalline (has a highly ordered atomic structure) as opposed to amorphous (lacks long-range atomic order) [95]. The degree of crystallinity can vary depending on the material and the processing conditions [95]. Pure silver is a highly crystalline metal, with a typical degree of crystallinity close to 100.0 % [59]. Pure copper is also highly crystalline, with a typical degree of crystallinity around 98.0 % [60]. Pure titanium is a crystalline metal, but its degree of crystallinity can vary depending on the processing conditions. Typically, the degree of crystallinity for pure titanium is around 90.0 % [61]. For highly pure and well-processed metals, the percentage of crystallinity can approach 100.0 % [102]. However, in practical applications, it's rare to achieve complete crystallinity due to factors like impurities, defects, and processing conditions [62].

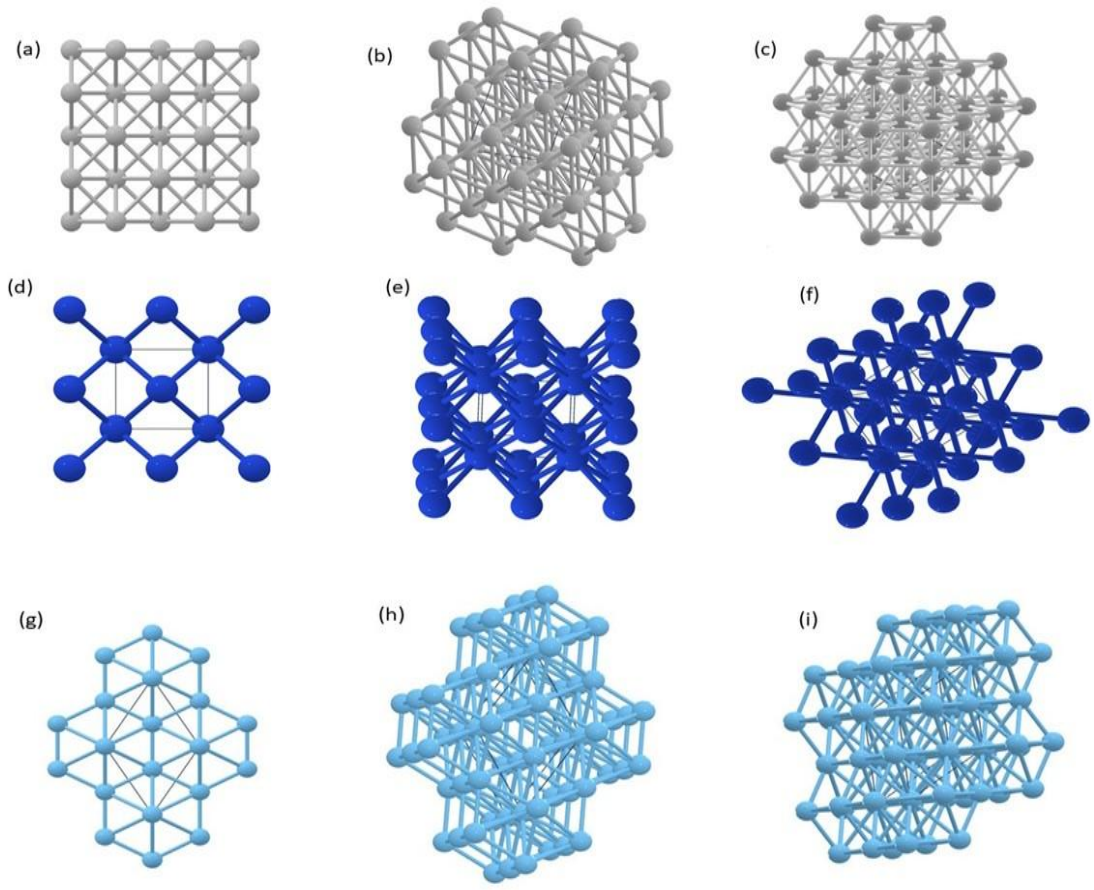

Fig.2. (a), (b), (c) crystal structure of silver (Ag) is face-centered cubic (FCC); (d), (e), (f) copper (Cu) crystal structure is face-centered cubic (FCC).; (g), (h), (i) crystal structure of titanium (Ti) is hexagonal close-packed (HCP). [63].

The preferred orientation, also known as texture or crystallographic texture, of a material, refers to the preferential alignment of crystallites (grains) in a particular direction relative to the sample's geometry or processing conditions [96]. The preferred orientation can significantly influence the material's properties, such as mechanical strength, electrical conductivity, and corrosion resistance [64]. Here's a comparative overview of the preferred orientation of Ag, Cu, and Ti crystals. Silver crystals typically exhibit a strong preferred orientation in the (111) direction when deposited as thin films or coatings [65]. This favored alignment is due to the reduced surface energy of the (111) plane within the face-centered cubic (FCC) arrangement of

silver[65]. The (111) texture can enhance the electrical conductivity and overall performance of silver in electronic and optoelectronic applications. Like silver, copper also has an FCC crystal structure, and it tends to develop a preferred orientation along the (111) direction when deposited as thin films or coatings [66]. On the other hand, titanium possesses a crystal structure that is hexagonally close-packed (HCP), and its preferred orientation can vary depending on the processing conditions and the specific application. In many cases, titanium exhibits a strong (0002) basal plane texture, which is beneficial for enhancing mechanical properties like strength and fatigue resistance [67]. Overall, while silver and copper tend to exhibit a strong (111) texture due to their FCC structure, titanium's preferred orientation is more dependent on the specific processing conditions and application requirements, with the (0002) basal plane texture being commonly observed [97].

4.1.1 Lattice Strain and Lattice Volume Analysis

The lattice strain in a crystal structure is a measure of the deformation or distortion of the crystal lattice from its ideal, unstrained configuration [98]. The lattice strain can arise due to various factors, such as the presence of impurities, defects, or external forces applied to the crystal [68]. To compare the lattice strain values of Ag, Cu and Ti crystals, we need to consider their crystal structures and the factors that contribute to lattice strain in each case. Lattice parameter (a) for Ag: 4.0862 Å (at 25.0 °C) [69]. The lattice strain of Ag was determined to be 0.00219 % in previous research [105]. The lattice strain in silver can occur due to factors such as impurities or dislocations. However, it's generally low due to the close-packed arrangement of atoms in its FCC structure [99]. Generally, silver has a relatively low lattice strain due to its high ductility and ability to accommodate deformations. On the other hand, Lattice parameter (a) for Cu: 3.6150 Å (at 25.0°C) [71]. The lattice strain of Cu was determined to be 1.39 % in previous research [103]. Cu is also a ductile metal, but it may exhibit slightly higher lattice strain

compared to silver due to its higher stacking fault energy and higher propensity for forming dislocations [104]. Again, lattice parameters (a and c) for Ti: 2.9506 Å and 4.6855 Å (at 25.0°C) respectively for HCP Ti [71]. In the hexagonally close-packed (HCP) crystal structure of titanium (Ti), the conventional lattice strain is often described using the c/a ratio, which is the ratio of the lattice parameters c (the height of the unit cell) and a (the edge length of the basal plane). The standard or commonly accepted c/a ratio for titanium is: (c/a) Ti ≈ 1.587 % [101]. Titanium generally exhibits higher lattice strain compared to Ag and Cu due to its crystal structure and lower ductility (**Fig. 3)** [100]. In the hexagonal close-packed (HCP) phase, which remains stable at room temperature, the lattice strain may be notable owing to the hexagonal packing configuration. However, at elevated temperatures, Ti can adopt a BCC structure with lower lattice strain [54].

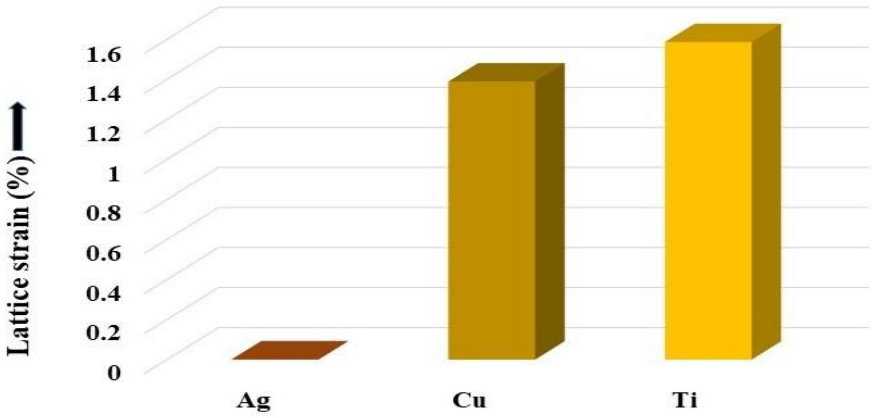

Fig. 3. Lattice strain curve of Ag, Cu and Ti crystals.

The lattice volume of a crystal denotes the volume occupied by the unit cell within its crystal lattice arrangement. It is determined by the size of the unit cell and the arrangement of atoms within it [72]. To compare the lattice volumes of Ag, Cu, and Ti crystals, we need to know their crystal structures and lattice parameters. The lattice volume correlates directly with both the crystal structure and the lengths of the unit cell edges. For Ag, lattice volume (V) = a^3 = (4.0862

Å)^3 = 68.30 Å^3 [73]; for Cu, lattice volume (V) = a^3 = (3.6150 Å)^3 = 47.23 Å^3 [74]; for Ti, lattice volume (V) = (0.866 × a^2 × c) = (0.866 × (2.9506 Å)^2 × 4.6855 Å) = 35.10 Å^3 [75]. Based on the calculations, the order of the lattice volumes from largest to smallest is: Ag (FCC) > Cu (FCC) > Ti (HCP) (**Fig. 4)**.

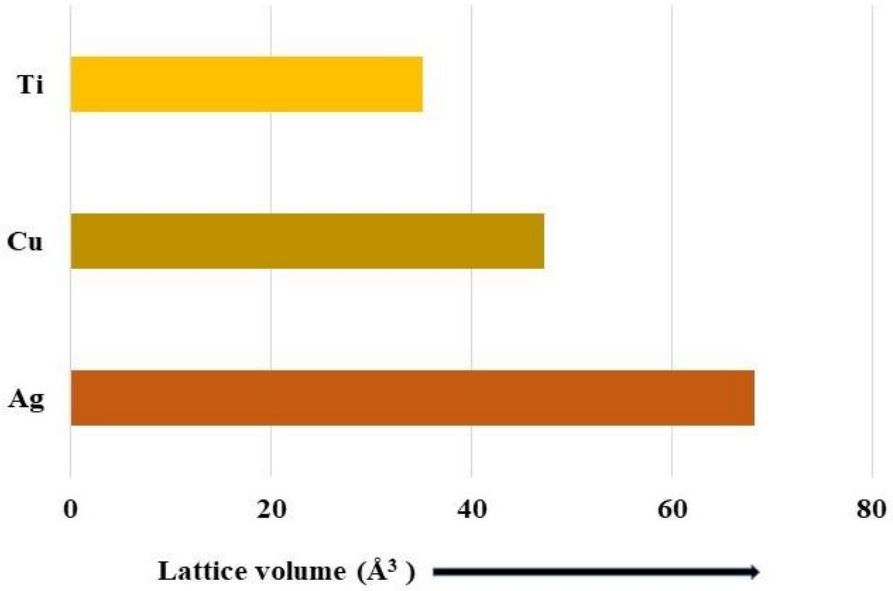

Fig. 4. Lattice volume curve of Ag, Cu and Ti crystals.

The lattice volume of silver (Ag) is the largest at 68.30 Å^3, followed by copper (Cu) at 47.23 Å^3, and titanium (Ti) has the smallest lattice volume of 35.10 Å^3. The difference in lattice volumes is primarily due to the different atomic radii and crystal structures of these metals. The FCC structure of Ag and Cu results in larger lattice volumes compared to the HCP structure of Ti [76].

4.2 Transmission Electron Microscopic (TEM) Analysis

Fig. 5. Shows the internal morphology of the selected titanium, silver and copper nanoparticles. Here the titanium nanoparticles were mostly spherical with a unified distribution but no agglomeration [115] as well and the same result was found for silver nanomaterials [113].

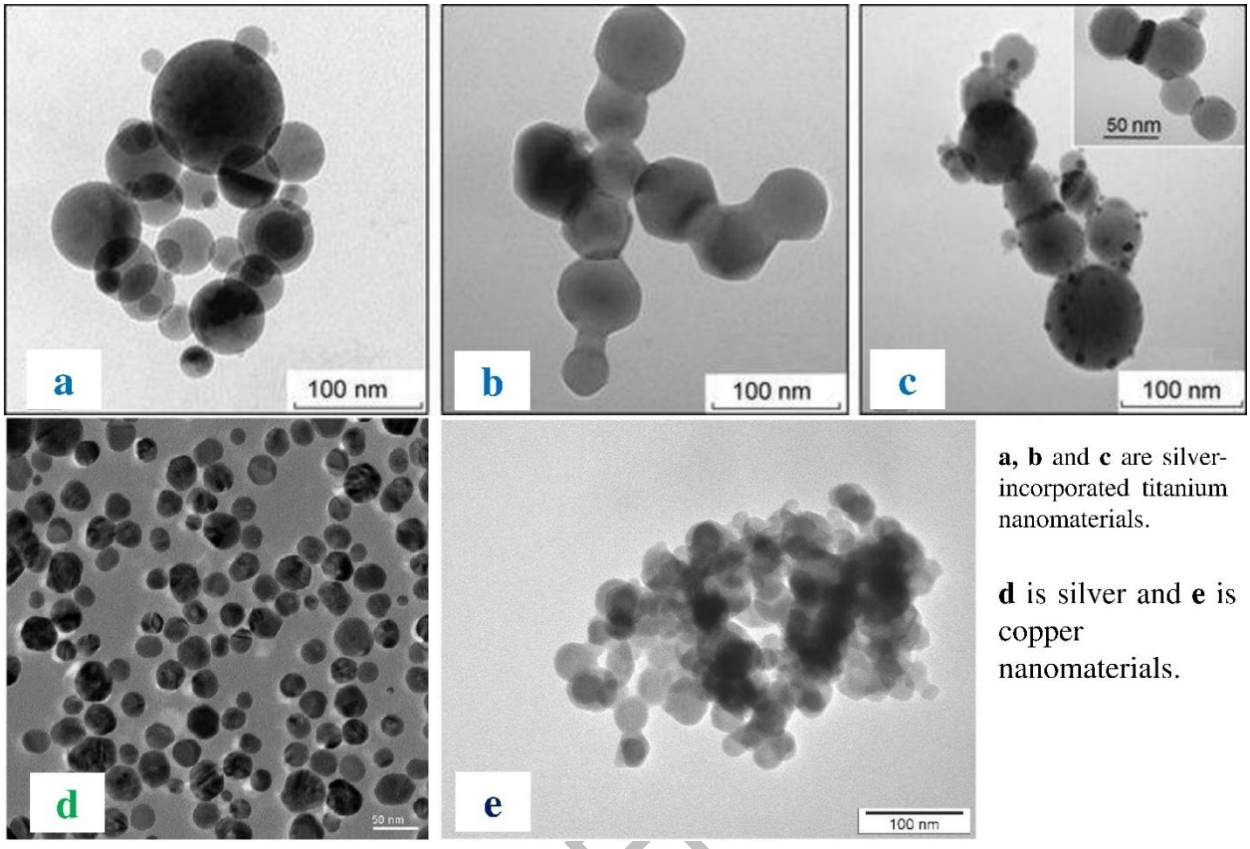

Fig. 5. Internal morphograph of (a), (b), (c) Ti [115]; (d) Ag [113] and (e) Cu [114] nanoparticles

On the other hand, the copper materials observed poor agglomerated and ball-shaped [114] nanoparticles. Fig. 6. Shows the diffraction plane of the nanocrystals by selected area electron diffraction (SAED). The crystalline predominant plane such as Miller indices observed in SAED [116-118] was revealed by XRD.

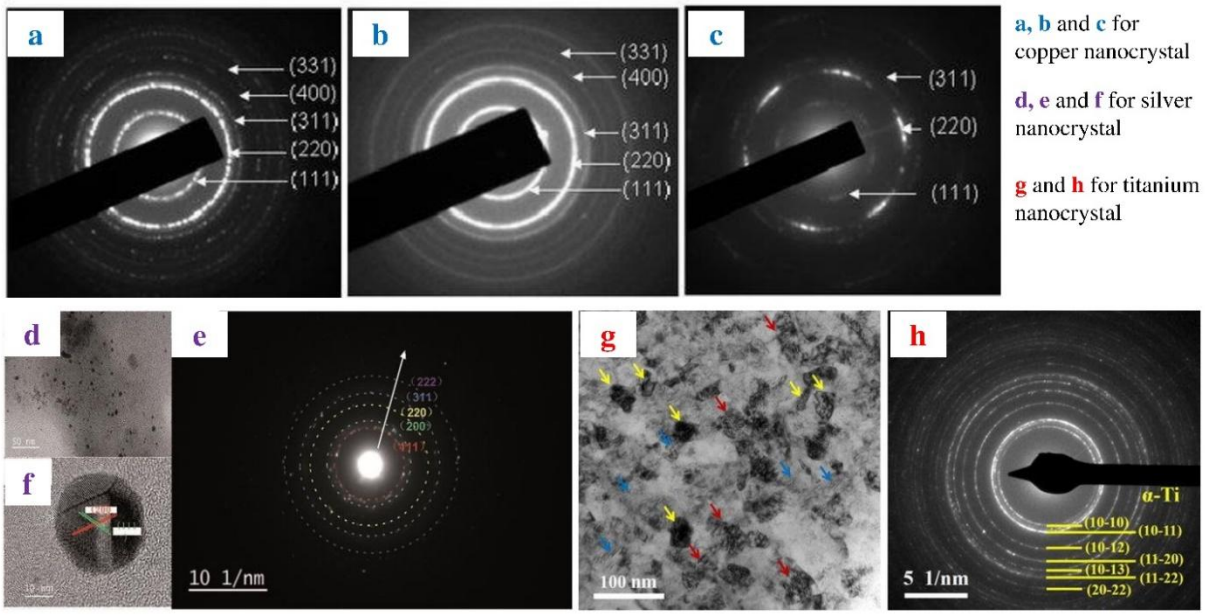

Fig. 6. Selected area electron diffraction pattern of Ag [116], Cu [117] and Ti [118] nanocrystals

Fig. 7. depicts the high-resolution TEM which showed the interplanar distance of the nanocrystals like Ag [119], Cu [120] and Ti [121]. The planes where the atoms were uniformly distributed and arranged an alignment of the atoms of Ag [119], Cu [120] and Ti [121].

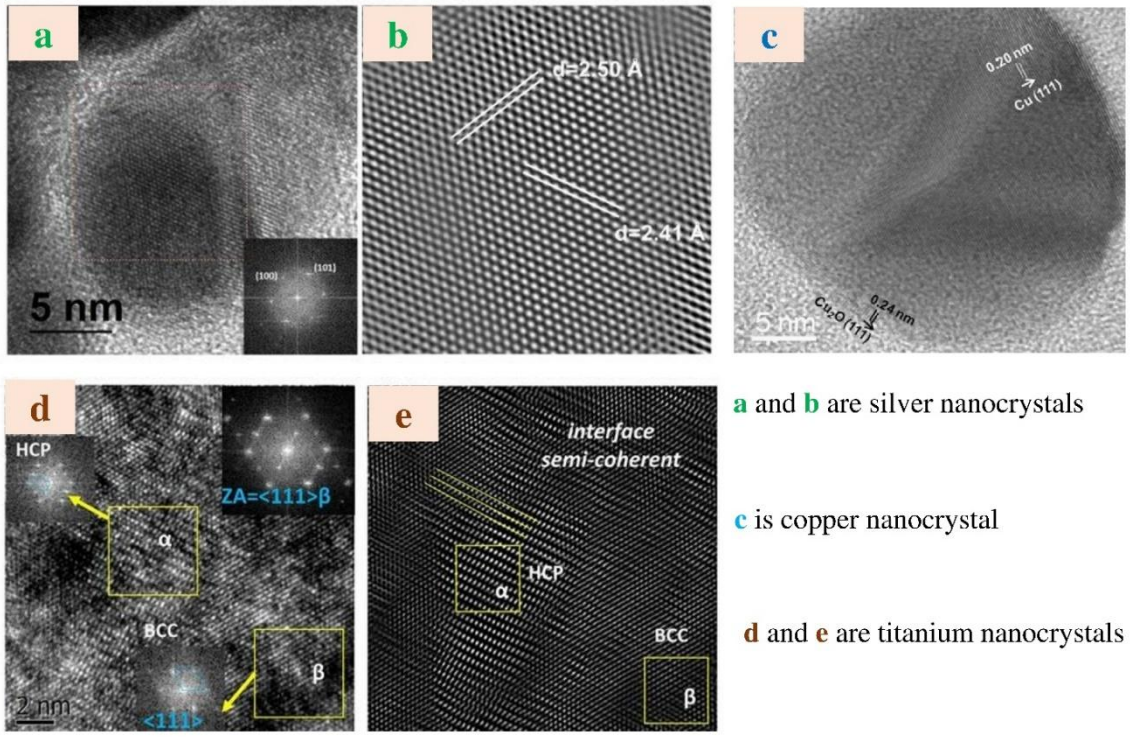

Fig. 7. HR-TEM of Ag [119], Cu [120] and Ti [121] nanocrystals

5.0 Comparative Overview of Ag, Cu and Ti nanocrystals Functional Applications

5.1 Electrical Conductivity

Among all metals, silver nanocrystals have the highest electrical conductivity. This property is attributed to the high mobility of electrons within the silver lattice, which results in the effective transmission of an electric current [106]. As a result, silver nanoparticles are common components of electronics, circuit parts, and high-performance conductive inks [77]. The second-best electrical conductor after silver is copper nanocrystals [107]. This metal resembles silver, as it has a high capability for the mobility of electrons [107]. Therefore, copper nanoparticles are used for electrical wires, power lines, and electrical motor manufacturing because of use for their low cost and satisfactory conductivity [78]. Titanium nanocrystals are not characterized by exceptional electrical conductivity. Despite the metal nature of titanium, it is a poor conductor in comparison to copper and silver [94]. Therefore, titanium nanocrystals are not widely used as conductive materials [79]. Nonetheless, titanium is used in industries where electrical conductibility is not a priority and other qualities, such as corrosion inhibition and biocompatibility, are preferred. These industries include aerospace and medical implant manufacturing [79].

5.2 Corrosion Resistance

The ability of silver nanocrystals to withstand corrosion is not well recognized. Although silver doesn't corrode in most situations, silver nanoparticles can undergo oxidation or other chemical reactions in specific situations [108]. To improve their durability and lessen the impacts of corrosion, silver nanoparticles are frequently coated all over the world [80]. On the other hand, copper nanocrystals are more likely to corrode, particularly in humid or acidic environments. Over time, copper oxidizes and develops a green patina, or copper oxide, on its surface [109]. However, copper nanocrystals can be made more corrosion-resistant by surface treatments or

alloying with other elements, which makes them useful for a variety of applications like electrical wire, roofing and plumbing [81]. The remarkable resistance to corrosion of titanium (Ti) nanocrystals is well known, especially in abrasive conditions like seawater and chemical processing. On its surface, titanium creates a protective oxide layer called titanium dioxide that stops more oxidation and corrosion [93]. Because of their intrinsic corrosion resistance, titanium (Ti) nanocrystals are widely sought after in applications such as biomedical implants, chemical processing equipment and marine structures where exposure to corrosive chemicals is a concern [82-83].

5.3 Catalytic Activity

Silver nanocrystals are renowned for their exceptional catalytic activity, particularly in oxidation reactions of organic compounds and alcohols [110]. Their high selectivity often leads to the formation of specific products, making them valuable in catalytic converters, environmental remediation, and chemical synthesis processes [84]. Cu nanocrystals, on the other hand, demonstrate versatile catalytic capabilities, participating in a wide range of reactions such as hydrogenation, dehydrogenation, and C-C coupling reactions [85]. Their excellent catalytic activity stems from their ability to engage in redox reactions, and they find applications in catalytic converters, carbon capture, fuel cells, and organic synthesis [111]. While less common as catalysts compared to silver and copper, Ti nanocrystals also exhibit catalytic activity in certain reactions, including hydrogenation, photocatalysis, and oxidation reactions [86]. Their selectivity can be influenced by factors such as surface morphology, crystal phase, and doping with other elements. Titanium nanocrystals are utilized in niche applications such as photocatalytic water splitting, environmental remediation, and the synthesis of fine chemicals [87].

5.4 Antimicrobial Property

Ag, Cu, and Ti nanocrystals possess distinctive antimicrobial properties, making them valuable in various applications ranging from healthcare to environmental remediation [112]. Ag nanocrystals are renowned for their potent antimicrobial activity, attributed to the release of silver ions (Ag^{+}) that interfere with bacterial cell membranes and DNA, inhibiting microbial growth [88, 116, 119]. This characteristic has resulted in the extensive utilization of silver nanoparticles in medical equipment, wound dressings, and antimicrobial coatings applied to surfaces [89]. Similarly, Cu nanocrystals exhibit strong antimicrobial efficacy due to the release of copper ions (Cu^{2+}) that disrupt microbial cell membranes and proteins, leading to cell death [90, 117, 120]. Cu nanoparticles find applications in healthcare settings, where they are used in hospital surfaces, door handles, and medical equipment to reduce the risk of healthcare-associated infections [91]. Ti nanocrystals, although less studied for their antimicrobial properties compared to silver and copper, also demonstrate antimicrobial activity through mechanisms such as photocatalysis and surface modification [92, 121].

Conclusion

This manuscript has presented a thorough crystallographic comparison of functional nanocrystals of silver, copper, and titanium using both transmission electron microscopy and X-ray diffraction techniques. By systematically analyzing data from a large number of studies, significant insights have been gained into the formation mechanisms and structural characteristics of these important nanomaterials. It has highlighted the key similarities and differences in the crystallography of the three nanocrystal systems. While all three metals can form a variety of crystalline phases and morphologies, subtle variations in synthetic parameters profoundly impact the resulting nanostructures. These crystallographic details, in turn, dictate the functional properties relevant to applications.

References

[1]. Kumar, R. (2021). Analysis and visualisation of research trends in nanomaterial: a general review. *Turkish Journal of Computer and Mathematics Education (TURCOMAT)*, *12*(2), 2959-2964.

[2]. Baig, N., Kammakakam, I., &Falath, W. (2021). Nanomaterials: A review of synthesis methods, properties, recent progress, and challenges. *Materials Advances*, *2*(6), 1821-1871.

[3]. Kang, J., Li, F., Xu, Z., Chen, X., Sun, M., Li, Y., ... & Guo, L. (2023). How Amorphous Nanomaterials Enhanced Electrocatalytic, SERS, and Mechanical Properties. *JACS Au*, *3*(10), 2660-2676.

[4]. Ramli, N. H., Nor, N. M., Hakimi, A., Zakaria, N. D., Lockman, Z., & Razak, K. A. (2024). Platinum-based Nanoparticles: A Review of Synthesis Methods, Surface Functionalization, and Their Applications. *Microchemical Journal*, 110280.

[5]. Ghosh, S., Sagayam, K. M., Haldar, D., Jone, A. A. A., Acharya, B., Gerogiannis, V. C., & Kanavos, A. (2024). A review on the types of nanomaterials and methodologies used for the development of biosensors. *Advances in Natural Sciences: Nanoscience and Nanotechnology*, *15*(1), 013001.

[6]. Xu, Y., Fang, X., & Zhang, Z. (2009). Formation of single-crystalline TiO2 nanomaterials with controlled phase composition and morphology and the application in dye-sensitized solar cell. *Applied Surface Science*, *255*(21), 8743-8749.

[7]. Bykkam, S., Ahmadipour, M., Narisngam, S., Kalagadda, V. R., &Chidurala, S. C. (2015). Extensive studies on X-ray diffraction of green synthesized silver nanoparticles. *Adv. Nanopart*, *4*(1), 1-10.

[8]. Alshareef, A. (2019). *An investigation into the effects of shape and structure on the antibacterial efficacy of metal nanoparticles* (Doctoral dissertation, De Montfort University).

[9]. Li, W. K., Gong, X. Q., Lu, G., &Selloni, A. (2008). Different reactivities of TiO2 polymorphs: comparative DFT calculations of water and formic acid adsorption at anatase and brookite TiO2 surfaces. *The Journal of Physical Chemistry C*, *112*(17), 6594-6596.

[10]. Agrawal, S., Bhatt, M., Rai, S. K., Bhatt, A., Dangwal, P., & Agrawal, P. K. (2018). Silver nanoparticles and its potential applications: A review. *Journal of Pharmacognosy and Phytochemistry*, *7*(2), 930-937.

[11]. Ghanghas, P., Jangid, N. K., &Poonia, K. (2023). Advanced Composites of Nanomaterials and Their Applications. In *Advanced Composites* (pp. 37-58). Cham: Springer Nature Switzerland.

[12]. Kang, D. K., Moon, S. K., Oh, K. T., Choi, G. S., & Kim, K. N. (2009). Properties of experimental titanium- silver- copper alloys for dental applications. *Journal of Biomedical Materials Research Part B: Applied Biomaterials*, *90*(1), 446-451.

[13]. Alavi, M., & Karimi, N. (2018). Characterization, antibacterial, total antioxidant, scavenging, reducing power and ion chelating activities of green synthesized silver, copper and titanium dioxide nanoparticles using Artemisia haussknechtii leaf extract. *Artificial cells, nanomedicine, and biotechnology*, *46*(8), 2066-2081.

[14]. Wysocka, I., Kowalska, E., Ryl, J., Nowaczyk, G., & Zielińska-Jurek, A. (2019). Morphology, photocatalytic and antimicrobial properties of TiO2 modified with mono-and bimetallic copper, platinum and silver nanoparticles. *Nanomaterials*, *9*(8), 1129.

[15]. Dikshit, P. K., Kumar, J., Das, A. K., Sadhu, S., Sharma, S., Singh, S., ... & Kim, B. S. (2021). Green synthesis of metallic nanoparticles: Applications and limitations. *Catalysts*, *11*(8), 902.

[16]. Charitidis, C. A., Georgiou, P., Koklioti, M. A., Trompeta, A. F., & Markakis, V. (2014). Manufacturing nanomaterials: from research to industry. *Manufacturing Review*, *1*, 11.

[17]. Kiran, J. U., Roners, J. P., & Mathew, S. (2020). XPS and thermal studies of silver doped SiO2 matrices for plasmonic applications. *Materials Today: Proceedings*, *33*, 1263-1267.

[18]. Ahmed, F., Kanoun, M. B., Awada, C., Jonin, C., & Brevet, P. F. (2021). An experimental and theoretical study on the effect of silver nanoparticle concentration on the structural, morphological, optical, and electronic properties of TiO2 nanocrystals. *Crystals*, *11*(12), 1488.

[19]. García, D. A., Mendoza, L., Vizuete, K., Debut, A., Arias, M. T., Gavilanes, A., ... &Dahoumane, S. A. (2020). Sugar-mediated green synthesis of silver selenide semiconductor nanocrystals under ultrasound irradiation. *Molecules*, *25*(21), 5193.

[20]. Torres-Flores, E. I., Flores-López, N. S., Martínez-Núñez, C. E., Tánori-Córdova, J. C., Flores-Acosta, M., & Cortez-Valadez, M. (2021). Silver nanoparticles in natural zeolites incorporated into commercial coating: antibacterial study. *Applied Physics A*, *127*, 1-11.

[21]. Yu, W., Xie, H., Chen, L., Li, Y., & Zhang, C. (2009). Synthesis and characterization of monodispersed copper colloids in polar solvents. *Nanoscale research letters*, *4*, 465-470.

[22]. LaGrow, A. P., Sinatra, L., Elshewy, A., Huang, K. W., Katsiev, K., Kirmani, A. R., ... & Bakr, O. M. (2014). Synthesis of copper hydroxide branched nanocages and their transformation to copper oxide. *The Journal of Physical Chemistry C*, *118*(33), 19374-19379.

[23]. Dharmadasa, R., Jha, M., Amos, D. A., & Druffel, T. (2013). Room temperature synthesis of a copper ink for the intense pulsed light sintering of conductive copper films. *ACS applied materials & interfaces*, *5*(24), 13227-13234.

[24]. Zhu, H. T., Zhang, C. Y., & Yin, Y. S. (2004). Rapid synthesis of copper nanoparticles by sodium hypophosphite reduction in ethylene glycol under microwave irradiation. *Journal of Crystal Growth*, *270*(3-4), 722-728.

[25]. Moghimi-Rad, J., Zabihi, F., Hadi, I., Ebrahimi, S., Isfahani, T. D., &Sabbaghzadeh, J. (2010). Effect of ultrasound radiation on the size and size distribution of synthesized copper particles. *Journal of Materials Science*, *45*(14), 3804-3811.

[26]. Wang, Y. N., Duan, X., Zheng, J., Lin, H., Yuan, Y., Ariga, H., ... & Asakura, K. (2012). Remarkable enhancement of Cu catalyst activity in hydrogenation of dimethyl oxalate to ethylene glycol using gold. *Catalysis Science & Technology*, *2*(8), 1637-1639.

[27]. Sugimoto, T., Zhou, X., & Muramatsu, A. (2003). Synthesis of uniform anatase TiO2 nanoparticles by gel–sol method: 3. Formation process and size control. *Journal of colloid and interface science*, *259*(1), 43-52.

[28]. Tripathi, A. K., Mathpal, M. C., Kumar, P., Singh, M. K., Mishra, S. K., Srivastava, R. K., ... & Agarwal, A. (2014). Synthesis-based structural and optical behavior of anatase TiO2 nanoparticles. *Materials Science in Semiconductor Processing*, *23*, 136-143.

[29]. Thapa, R., Maiti, S., Rana, T. H., Maiti, U. N., & Chattopadhyay, K. K. (2012). Anatase TiO2 nanoparticles synthesis via simple hydrothermal route: Degradation of Orange II, Methyl Orange and Rhodamine B. *Journal of Molecular Catalysis A: Chemical*, *363*, 223-229.

[30]. Kong, W., Chen, C., Mai, K., Shi, X., Hu, R., & Wang, Z. (2011). Large-scale synthesis and self-assembly of monodisperse spherical TiO2nanocrystals. *Journal of Nanomaterials*, *2011*, 1-4.

[31]. Mazhar, F., Kausar, A., & Iqbal, M. (2022). Photocatalytic hydrogen generation using TiO2: a state-of-the-art review. *Zeitschrift für Physikalische Chemie*, *236*(11-12), 1697-1728.

[32]. Ahamed, M. S., Ali, M. S., Ahmed, S., Sadia, S. I., Islam, M. R., Rahaman, M. A., & Alam, M. A. (2024). Synthesis of Silver Nanomaterials Capping by Fruit-mediated Extracts and Antimicrobial Activity: A Critical Review. *International Research Journal of Pure and Applied Chemistry*, *25*(1), 45-60.

[33]. Tabassum, M., Alam, M. A., Mostofa, S., Bishwas, R. K., Sarkar, D., & Jahan, S. A. (2024). Synthesis and crystallinity integration of copper nanoparticles by reaction medium. *Journal of Crystal Growth*, *626*, 127486.

[34]. Alam, M. A., Bishwas, R. K., Mostofa, S., & Jahan, S. A. (2024). Low-temperature synthesis and crystal growth behaviour of nanocrystal anatase-TiO2. *Materials Letters*, *354*, 135396.

[35]. Alam, M. A., Tabassum, M., Mostofa, S., Bishwas, R. K., Sarkar, D., & Jahan, S. A. (2023). The effect of precursor concentration on the crystallinity synchronization of synthesized copper nanoparticles. *Journal of Crystal Growth*, *621*, 127386.

[36]. Alam, M. A., Mobashsara, M. T., Sabrina, S. M., Bishwas, R. K. B., Debasish, D. S., & Shirin, S. A. J. (2023). One-pot low-temperature synthesis of high crystalline cu nanoparticles. *Malaysian Journal of Science and Advanced Technology*, 122-127.

[37]. Alam, M. A., Munni, S. A., Mostafa, S., Bishwas, R. K., & Jahan, S. A. (2023). An investigation on a synthesis of silver nanoparticles. *Asian Journal of Research in Biochemistry*, *12*(3), 1-10.

[38]. Giannini, C., Ladisa, M., Altamura, D., Siliqi, D., Sibillano, T., & De Caro, L. (2016). X-ray diffraction: a powerful technique for the multiple-length-scale structural analysis of nanomaterials. *Crystals*, *6*(8), 87.

[39]. Bushell, M., Beauchemin, S., Kunc, F., Gardner, D., Ovens, J., Toll, F., ... & Johnston, L. J. (2020). Characterization of commercial metal oxide nanomaterials: crystalline phase, particle size and specific surface area. *Nanomaterials*, *10*(9), 1812.

[40]. Gharibshahi, L., Saion, E., Gharibshahi, E., Shaari, A. H., &Matori, K. A. (2017). Structural and optical properties of Ag nanoparticles synthesized by thermal treatment method. *Materials*, *10*(4), 402.

[41]. Mahdieh, M., Zolanvari, A., &Azimee, A. S. (2012). Green biosynthesis of silver nanoparticles by Spirulina platensis. *Scientia Iranica*, *19*(3), 926-929.

[42].Pathak, T. K., Kroon, R. E., & Swart, H. C. (2018). Photocatalytic and biological applications of Ag and Au doped ZnO nanomaterial synthesized by combustion. *Vacuum*, *157*, 508-513.

[43].Babu, M. G., & Gunasekaran, P. (2009). Production and structural characterization of crystalline silver nanoparticles from Bacillus cereus isolate. *Colloids and surfaces B: Biointerfaces*, *74*(1), 191-195.

[44].Forough, M., & Farhadi, K. (2010). Biological and green synthesis of silver nanoparticles. *Turkish J. Eng. Env. Sci*, *34*(4), 281-287.

[45].Shameli, K., Bin Ahmad, M., Jaffar Al-Mulla, E. A., Ibrahim, N. A., Shabanzadeh, P., Rustaiyan, A., ... & Zidan, M. (2012). Green biosynthesis of silver nanoparticles using Callicarpa maingayi stem bark extraction. *Molecules*, *17*(7), 8506-8517.

[46].Al-thabaiti, S. A., Obaid, A. Y., Khan, Z., Bashir, O., & Hussain, S. (2015). Cu nanoparticles: synthesis, crystallographic characterization, and stability. *Colloid and Polymer Science*, *293*, 2543-2554.

[47].Tabassum, M., Alam, M. A., Mostofa, S., Bishwas, R. K., Sarkar, D., & Jahan, S. A. (2024). Synthesis and crystallinity integration of copper nanoparticles by reaction medium. *Journal of Crystal Growth*, *626*, 127486.

[48].Alam, M. A., Mobashsara, M. T., Sabrina, S. M., Bishwas, R. K. B., Debasish, D. S., & Shirin, S. A. J. (2023). One-pot low-temperature synthesis of high crystalline cu nanoparticles. *Malaysian Journal of Science and Advanced Technology*, 122-127.

[49].Khan, A., Rashid, A., Younas, R., & Chong, R. (2016). A chemical reduction approach to the synthesis of copper nanoparticles. *International Nano Letters*, *6*, 21-26.

[50].Li, H., & Cai, W. (2018). Understanding the deformation mechanism of individual phases of a dual-phase beta type titanium alloy using in situ diffraction method. *Materials Science and Engineering: A*, *728*, 151-156.

[51].Yan, M., Luo, S. D., Schaffer, G. B., & Qian, M. (2012). TEM and XRD characterisation of commercially pure α-Ti made by powder metallurgy and casting. *Materials letters*, *72*, 64-67.

[52].Gemelli, E., & Camargo, N. H. A. (2007). Oxidation kinetics of commercially pure titanium. *Matéria (Rio de Janeiro)*, *12*, 525-531.

[53].Bieler, T. R., Wang, L., Beaudoin, A. J., Kenesei, P., & Lienert, U. (2014). In situ characterization of twin nucleation in pure Ti using 3D-XRD. *Metallurgical and Materials Transactions A*, *45*, 109-122.

[54].Kolli, R. P., & Devaraj, A. (2018). A review of metastable beta titanium alloys. *Metals*, *8*(7), 506.

[55].Ghosh, A., Singh, A., & Gurao, N. P. (2017). Effect of rolling mode and annealing temperature on microstructure and texture of commercially pure-titanium. *Materials Characterization*, *125*, 83-93.

[56].Mabrouk, M. M., Mansour, A. T., Abdelhamid, A. F., Abualnaja, K. M., Mamoon, A., Gado, W. S., ... & Ayoub, H. F. (2021). Impact of aqueous exposure to silver nanoparticles on growth performance, redox status, non-specific immunity, and histopathological changes of Nile Tilapia, Oreochromis niloticus, challenged with Aeromonas hydrophila. *Aquaculture Reports*, *21*, 100816.

[57].Phul, R., Kaur, C., Farooq, U., & Ahmad, T. (2018). Ascorbic acid assisted synthesis, characterization and catalytic application of copper nanoparticles. *Mater. Sci. Eng. Int. J*, *2*(4), 90-94.

[58].Balbinotti, P., Gemelli, E., Buerger, G., Lima, S. A. D., Jesus, J. D., Camargo, N. H. A., ... & Soares, G. D. D. A. (2011). Microstructure development on sintered Ti/HA biocomposites produced by powder metallurgy. *Materials Research*, *14*, 384-393.

[59].Zhong, J., Zhang, L. H., Jin, Z. H., Sui, M. L., & Lu, K. (2001). Superheating of Ag nanoparticles embedded in Ni matrix. *Acta materialia*, *49*(15), 2897-2904.

[60].Sastry, A. B. S., Karthik Aamanchi, R. B., Sree Rama Linga Prasad, C., & Murty, B. S. (2013). Large-scale green synthesis of Cu nanoparticles. *Environmental chemistry letters*, *11*, 183-187.

[61].Abe, Y., Matsui, E., & Senna, M. (2007). Preparation of phase pure and well-crystallized Li4Ti5O12 nanoparticles by precision control of starting mixture and calcining at lowest possible temperatures. *Journal of Physics and Chemistry of Solids*, *68*(5-6), 681-686.

[62].Pang, Y. X., & Bao, X. (2003). Influence of temperature, ripening time and calcination on the morphology and crystallinity of hydroxyapatite nanoparticles. *Journal of the European Ceramic Society*, *23*(10), 1697-1704.

[63].Jain, A., Ong, S. P., Hautier, G., Chen, W., Richards, W. D., Dacek, S., ... & Persson, K. A. (2013). Commentary: The Materials Project: A materials genome approach to accelerating materials innovation. *APL materials*, *1*(1).

[64].Kamb, W. B. (1959). Theory of preferred crystal orientation developed by crystallization under stress. *The Journal of Geology*, *67*(2), 153-170.

[65].Pan, H., Sun, H., Poh, C., Feng, Y., & Lin, J. (2005). Single-crystal growth of metallic nanowires with preferred orientation. *Nanotechnology*, *16*(9), 1559.

[66].Wang, Y., Ghanbaja, J., Soldera, F., Boulet, P., Horwat, D., Mücklich, F., & Pierson, J. F. (2014). Controlling the preferred orientation in sputter-deposited Cu2O thin films: Influence of the initial growth stage and homoepitaxial growth mechanism. *Acta materialia*, *76*, 207-212.

[67].Keeler, J. H., & Geisler, A. H. (1956). Preferred orientations in rolled and annealed titanium. *JOM*, *8*(2), 80-90.

[68].Miao, Y., Zhao, Y., Zhang, S., Shi, R., & Zhang, T. (2022). Strain engineering: a boosting strategy for photocatalysis. *Advanced Materials*, *34*(29), 2200868.

[69].Sun, Y., Ren, Y., Liu, Y., Wen, J., Okasinski, J. S., & Miller, D. J. (2012). Ambient-stable tetragonal phase in silver nanostructures. *Nature communications*, *3*(1), 971.

[70].Zheng, Y., Li, X., Cheng, X., Li, Z., Liu, Y., & Dong, C. (2018). Enhanced thermal stability of Cu alloy films by strong interaction between Ni and Zr (or Fe). *Journal of Physics D: Applied Physics*, *51*(13), 135304.

[71].Alloys, Z. S. M. H. S. (2013). First-principles Studies on the Structures and Properties of Ti-and.

[72].Tilley, R. J. (2020). *Crystals and crystal structures*. John Wiley & Sons.

[73].Yamamura, A., Maruoka, S., Ohtsuka, J., Miyakawa, T., Nagata, K., Kataoka, M., ... &Tanokura, M. (2009). Expression, purification, crystallization and preliminary X-ray analysis of conjugated polyketone reductase C2 (CPR-C2) from Candida parapsilosis IFO 0708. *Acta Crystallographica Section F: Structural Biology and Crystallization Communications*, *65*(11), 1145-1148.

[74].Hebbaz, A., Belhani, M., & Tahraoui, T. (2024). Synthesis of cerium-doped magnesium spinel ferrites and study of their physical properties for photocatalytic applications under sunlight irradiation. *Applied Physics A*, *130*(2), 1-14.

[75].Gupta, R., Kim, E. Y., Shin, H. S., Lee, G. Y., & Yeo, D. H. (2023). Structural, microstructural, and microwave dielectric properties of (Al1-xBx) 2Mo3O12 ceramics with low dielectric constant and low dielectric loss for LTCC applications. *Ceramics International*, *49*(14), 22690-22701.

[76].Manna, I., Chattopadhyay, P. P., Nandi, P., Banhart, F., & Fecht, H. J. (2003). Formation of face-centered-cubic titanium by mechanical attrition. *Journal of Applied Physics*, *93*(3), 1520-1524.

[77].Mahendia, S., Tomar, A. K., & Kumar, S. (2010). Electrical conductivity and dielectric spectroscopic studies of PVA–Ag nanocomposite films. *Journal of Alloys and Compounds*, *508*(2), 406-411.

[78].Sivasubramaniyam, V., Ramasamy, S., Venkatraman, M., Gatto, G., & Kumar, A. (2023). Carbon Nanotubes as an Alternative to Copper Wires in Electrical Machines: A Review. *Energies*, *16*(9), 3665.

[79].Kaur, M., & Singh, K. (2019). Review on titanium and titanium based alloys as biomaterials for orthopaedic applications. *Materials Science and Engineering: C*, *102*, 844-862.

[80].Asaad, M. A., Ismail, M., Tahir, M. M., Huseien, G. F., Raja, P. B., & Asmara, Y. P. (2018). Enhanced corrosion resistance of reinforced concrete: Role of emerging eco-friendly Elaeisguineensis/silver nanoparticles inhibitor. *Construction and Building Materials*, *188*, 555-568.

[81].Bastidas, D. M., Criado, M., Fajardo, S., La Iglesia, V. M., Cano, E., & Bastidas, J. M. (2010). Copper deterioration: causes, diagnosis and risk minimisation. *International materials reviews*, *55*(2), 99-127.

[82].Al Othman, Z. A., Alam, M. M., Naushad, M., Inamuddin, I., & Khan, M. F. (2013, July). Inorganic nanoparticles and nanomaterials based on titanium (Ti): applications in medicine. In *Materials Science Forum* (Vol. 754, pp. 21-87). Trans Tech Publications Ltd.

[83].Zhang, L. C., Chen, L. Y., & Wang, L. (2020). Surface modification of titanium and titanium alloys: technologies, developments, and future interests. *Advanced Engineering Materials*, *22*(5), 1901258.

[84].Dong, X. Y., Gao, Z. W., Yang, K. F., Zhang, W. Q., & Xu, L. W. (2015). Nanosilver as a new generation of silver catalysts in organic transformations for efficient synthesis of fine chemicals. *Catalysis Science & Technology*, *5*(5), 2554-2574.

[85].Gawande, M. B., Goswami, A., Felpin, F. X., Asefa, T., Huang, X., Silva, R., ... & Varma, R. S. (2016). Cu and Cu-based nanoparticles: synthesis and applications in catalysis. *Chemical reviews*, *116*(6), 3722-3811.

[86].Jeon, J. P., Kweon, D. H., Jang, B. J., Ju, M. J., & Baek, J. B. (2020). Enhancing the photocatalytic activity of TiO2 catalysts. *Advanced Sustainable Systems*, *4*(12), 2000197.

[87].Ma, Y., Wang, X., Jia, Y., Chen, X., Han, H., & Li, C. (2014). Titanium dioxide-based nanomaterials for photocatalytic fuel generations. *Chemical reviews*, *114*(19), 9987-10043.

[88].Le Ouay, B., &Stellacci, F. (2015). Antibacterial activity of silver nanoparticles: A surface science insight. *Nano today*, *10*(3), 339-354.

[89].Knetsch, M. L., & Koole, L. H. (2011). New strategies in the development of antimicrobial coatings: the example of increasing usage of silver and silver nanoparticles. *Polymers*, *3*(1), 340-366.

[90].Milojkov, D. V., Radosavljević-Mihajlović, A. S., Stanić, V. D., Nastasijević, B. J., Radotić, K., Janković-Častvan, I., & Živković-Radovanović, V. (2023). Synthesis and characterization of luminescent Cu2+–doped fluorapatite nanocrystals as potential broad–spectrum antimicrobial agents. *Journal of Photochemistry and Photobiology B: Biology*, *239*, 112649.

[91].Bisht, N., Dwivedi, N., Kumar, P., Venkatesh, M., Yadav, A. K., Mishra, D., ... & Dhand, C. (2022). Recent advances in copper and copper-derived materials for antimicrobial resistance and infection control. *Current Opinion in Biomedical Engineering*, *24*, 100408.

[92].Chouirfa, H., Bouloussa, H., Migonney, V. U., & Falentin-Daudré, C. (2019). Review of titanium surface modification techniques and coatings for antibacterial applications. *Acta biomaterialia*, *83*, 37-54.

[93].Das, R., Ambardekar, V., & Bandyopadhyay, P. P. (2021). *Titanium dioxide and its applications in mechanical, electrical, optical, and biomedical fields* (Vol. 7). London, UK: IntechOpen.

[94].Gulbiński, W., Suszko, T., Sienicki, W., &Warcholiński, B. (2003). Tribological properties of silver-and copper-doped transition metal oxide coatings. *Wear*, *254*(1-2), 129-135.

[95].Cheng, Y. Q., & Ma, E. (2011). Atomic-level structure and structure–property relationship in metallic glasses. *Progress in materials science*, *56*(4), 379-473.

[96].Wenk, H. R. (Ed.). (2013). *Preferred orientation in deformed metal and rocks: an introduction to modern texture analysis*. Elsevier.

[97].Lütjering, G., Williams, J. C., & Gysler, A. (2000). Microstructure and mechanical properties of titanium alloys. In *Microstructure And Properties Of Materials: (Volume 2)* (pp. 1-77).

[98].Withers, P. J., Preuss, M., Steuwer, A., & Pang, J. (2007). Methods for obtaining the strain-free lattice parameter when using diffraction to determine residual stress. *Journal of applied crystallography*, *40*(5), 891-904.

[99].Smallman, R. E., & Bishop, R. J. (2013). *Metals and materials: science, processes, applications*. Elsevier.

[100].Warwick, J. L. W., Jones, N. G., Rahman, K. M., & Dye, D. (2012). Lattice strain evolution during tensile and compressive loading of CP Ti. *Acta Materialia*, *60*(19), 6720-6731.

[101].Nan, X. L., Wang, H. Y., Wu, Z. Q., Xue, E. S., Zhang, L., & Jiang, Q. C. (2013). Effect of c/a axial ratio on Schmid factors in hexagonal close-packed metals. *Scripta Materialia*, *68*(7), 530-533.

[102].Zhang, J. P., Liao, P. Q., Zhou, H. L., Lin, R. B., & Chen, X. M. (2014). Single-crystal X-ray diffraction studies on structural transformations of porous coordination polymers. *Chemical Society Reviews*, *43*(16), 5789-5814.

[103].Şelte, A., &Özkal, B. (2019). Crystallite size and strain calculations of hard particle reinforced composite powders (Cu/Ni/Fe–WC) synthesized via mechanical alloying. *Proceedings of the Estonian Academy of Sciences*, *68*(1), 66-78.

[104].Mara, N. A., & Beyerlein, I. J. (2014). effect of bimetal interface structure on the mechanical behavior of Cu–Nb fcc–bcc nanolayered composites. *Journal of materials science*, *49*, 6497-6516.

[105].Ali, M. H., Azad, M. A. K., Khan, K. A., Rahman, M. O., Chakma, U., & Kumer, A. (2023). Analysis of crystallographic structures and properties of silver nanoparticles synthesized using PKL extract and nanoscale characterization techniques. *ACS omega*, *8*(31), 28133-28142.

[106].Khalil, A. M., Hassan, M. L., & Ward, A. A. (2017). Novel nanofibrillated cellulose/polyvinylpyrrolidone/silver nanoparticles films with electrical conductivity properties. *Carbohydrate polymers*, *157*, 503-511.

[107].Hernandez-Castaneda, J. C., Lok, B. K., & Zheng, H. (2020). Laser sintering of Cu nanoparticles on PET polymer substrate for printed electronics at different wavelengths and process conditions. *Frontiers of Mechanical Engineering*, *15*, 303-318.

[108].Levard, C., Hotze, E. M., Lowry, G. V., & Brown Jr, G. E. (2012). Environmental transformations of silver nanoparticles: impact on stability and toxicity. *Environmental science & technology*, *46*(13), 6900-6914.

[109].Leygraf, C., Chang, T., Herting, G., &Wallinder, I. O. (2019). The origin and evolution of copper patina colour. *Corrosion Science*, *157*, 337-346.

[110].Dong, X. Y., Gao, Z. W., Yang, K. F., Zhang, W. Q., & Xu, L. W. (2015). Nanosilver as a new generation of silver catalysts in organic transformations for efficient synthesis of fine chemicals. *Catalysis Science & Technology*, *5*(5), 2554-2574.

[111].Dey, S., & Dhal, G. C. (2020). Controlling carbon monoxide emissions from automobile vehicle exhaust using copper oxide catalysts in a catalytic converter. *Materials Today Chemistry*, *17*, 100282.

[112].Makvandi, P., Wang, C. Y., Zare, E. N., Borzacchiello, A., Niu, L. N., & Tay, F. R. (2020). Metal- based nanomaterials in biomedical applications: antimicrobial activity and cytotoxicity aspects. *Advanced Functional Materials*, *30*(22), 1910021.

[113]. Chou, K. S., Huang, K. C., & Lee, H. H. (2005). Fabrication and sintering effect on the morphologies and conductivity of nano-Ag particle films by the spin coating method. *Nanotechnology*, *16*(6), 779.

[114]. Mroczek-Sosnowska, N., Sawosz, E., Vadalasetty, K. P., Łukasiewicz, M., Niemiec, J., Wierzbicki, M., ... &Chwalibog, A. (2015). Nanoparticles of copper stimulate angiogenesis at systemic and molecular level. *International journal of molecular sciences*, *16*(3), 4838-4849.

[115].Svarovskaya, N. V., Bakina, O. V., Pervikov, A. V., Rubtsov, K. V., & Lerner, M. I. (2020). Electrical Explosion of Wires for Manufacturing Bimetallic Antibacterial Ti–Ag and Fe–Ag Nanoparticles. *Russian Physics Journal*, *62*, 1580-1586.

[116]. Cai, Y., Piao, X., Gao, W., Zhang, Z., Nie, E., & Sun, Z. (2017). Large-scale and facile synthesis of silver nanoparticles via a microwave method for a conductive pen. *RSC advances*, *7*(54), 34041-34048.

[117]. Shen, H., Wang, H., Yuan, H., Ma, L., & Li, L. S. (2012). Size-, shape-, and assembly-controlled synthesis of Cu 2− x Se nanocrystals via a non-injection phosphine-free colloidal method. *CrystEngComm*, *14*(2), 555-560.

[118]. Zhang, B., Wang, J., Zhu, S., Zhu, N., Zhang, J., & Wang, Z. (2019). Effects of ECAP on the formation and tribological properties of thermal oxidation layers on a pure titanium surface. *Oxidation of Metals*, *91*, 483-494.

[119]. Virgen-Ortiz, A., Limón-Miranda, S., Soto-Covarrubias, M. A., Apolinar-Iribe, A., Rodríguez-León, E., & Iñiguez-Palomares, R. (2015). Biocompatible silver nanoparticles synthesized using rumexhymenosepalus extract decreases fasting glucose levels in diabetic rats. *Dig. J. Nanomater. Biostruct*, *10*(3), 927-933.

[120]. Cheng, G., & Hight Walker, A. R. (2010). Transmission electron microscopy characterization of colloidal copper nanoparticles and their chemical reactivity. *Analytical and bioanalytical chemistry*, *396*, 1057-1069.

[121]. Kou, W., Sun, Q., Xiao, L., & Sun, J. (2019). Superior plasticity stability and excellent strength in Ti-55531 alloy micropillars via harmony slip in nanoscale α/β phases. *Scientific Reports*, *9*(1), 5075.